Negative diffusion coefficient in a two-dimensional lattice-gas system with attractive nearest-neighbor interactions

P. Argyrakis,[1] A. A. Chumak,[2] M. Maragakis,[1] and N. Tsakiris[1]
[1]*Department of Physics, University of Thessaloniki, 54124 Thessaloniki, Greece*
[2]*Institute of Physics of the National Academy of Sciences, prospekt Nauki 46, Kyiv 03028, Ukraine*
(Received 8 May 2009; revised manuscript received 24 August 2009; published 30 September 2009)

Collective diffusion in a two-dimensional lattice-gas system undergoing first-order phase transition is studied both theoretically and by means of Monte Carlo (MC) simulations. The nearest-neighbor attractive interactions result in the formation of a two-phase mixture in which the characteristic size of the dense phase grows with time as $t^{1/3}$. It is shown analytically that the evolution of large-scale coverage inhomogeneities is governed by the diffusion equation with a negative diffusion coefficient. Similar to the phenomenon of Ostwald ripening, the Gibbs-Thompson effect is responsible for this abnormal diffusion. MC simulations of random jumps of individual particles also show the presence of negative diffusion caused by the macroscopically inhomogeneous distribution of particle density. The collective diffusion coefficients obtained both theoretically and by means of MC simulations are in satisfactory agreement.

DOI: 10.1103/PhysRevB.80.104203 PACS number(s): 64.60.−i, 68.35.Fx, 68.35.Rh, 05.50.+q

I. INTRODUCTION

A lattice-gas system with attractive nearest-neighbor interactions undergoes first-order phase transition when its temperature, T, is lower than the critical one, T_c. In this case, the statistically homogeneous system is transformed into a mixture of dense and dilute phases. The phase-separation process lasts for infinitely long time and manifests itself in an increase of characteristic lengths of the dense and dilute phases. Structural inhomogeneities at arbitrary time t are statistically similar to those at differing time, t', being scaled by some factor dependent on the time difference $t-t'$. Lifshitz and Slyozov in Ref. 1 (see also Ref. 2) were the first to describe theoretically the late stage of the two-phase evolution for the case of a three-dimensional (3D) system with a small volume fraction of the dense phase. It was shown that the characteristic size of dense droplets behaves as $t^{1/3}$. A similar dependence was also obtained for the two-dimensional (2D) case. While average radius of the droplets, $\bar{R}$, increases with time $[\bar{R}\sim t^{1/3}]$, their total number decreases: large droplets grow by the condensation of material diffused from small evaporated droplets. During this coarsening process, known in the literature as Ostwald ripening, the system evolves toward the state with minimum interfacial free energy which is proportional to $\bar{R}(t)^{-1}$.

The coarsening can be explained as follows. In close vicinity to a droplet of radius R, the particle concentration in the dilute phase, n^{di}, is slightly different from the value n_∞ corresponding to large R, $(R\to\infty)$. This phenomenon is known in the literature as the Gibbs-Thompson effect. The quantities n^{di} and R are related by

$$n^{di}(R) = n_\infty e^{\alpha/R}, \quad \frac{\alpha}{R} \ll 1. \tag{1}$$

Here α is the capillary length. Its explicit value can be expressed in terms of the lattice-gas parameters (see next section). As long as the individual droplets have different radii, the density of the dilute phase is not constant and there are local diffusion fluxes between them. It follows from Eq. (1) that the concentration n^{di} in the vicinity of small droplets is greater than the concentration near large droplets. Thus, mass transfer from small droplets toward large droplets (the "ripening" process) occurs. The "driving forces" giving rise to the local fluxes are proportional to the quantity α which in the literature is associated with the surface-tension coefficient.

Obviously, at any time t, there are specific droplets with $R=R^*$ which, on average, neither shrinking, nor growing during the characteristic times of particle redistribution between nearest droplets. The corresponding density of the dilute phase $n^{di}(R^*)=n_\infty \exp(\alpha/R^*)$ can also be considered as nearly stationary in contrast to the case of droplets with $R\neq R^*$. The local densities fluctuate around $n^{di}(R^*)$. Also, particle redistribution induced by local inhomogeneities occurs locally. Individual particles have low probability to execute long random-walk paths. In general, the effective paths for mass transport begin on the surface of one droplet and end on the surface of the nearest one with greater radius. We consider them to be of the order of the characteristic length of the dilute phase variation, i.e., of the order of the average distance between droplets, l. The value l can be estimated as $R^*/\theta^{1/2}$, where θ is the filling of the lattice sites averaged over both phases. For further analysis, it is convenient to define particle concentrations of the dense (n^{de}) and dilute (n^{di}) phases in the units of occupation probabilities (filling) of the corresponding lattice sites.

The question that arises is what will occur if one adds a small amount of particles, thus increasing their filling by $\delta\theta(\mathbf{r})$ ($\mathbf{r}$ is the lattice site coordinate). The characteristic length of $\delta\theta$ variations is assumed to be much greater than the interdroplet distance, l. How can the evolution of $\delta\theta$ be described? Obviously, fast redistribution of the excessive particles between nearest droplets should occur just after the deposition. Accordingly, $R^*(t,\theta)$ increases to the value $R^*(t,\theta+\delta\theta)$. Due to the dependence of $\delta\theta$ on $\mathbf{r}$, the quantities R^* and $n^{di}(R^*)$ also become dependent on $\mathbf{r}$. Moreover, it follows from Eq. (1) that, on average, the local density of the

 ©2009 The American Physical Society

dilute phase, $n^{di}(\mathbf{r})$, in the regions with small $\delta\theta$ becomes greater than that in the regions with high $\delta\theta$. This gives rise to a net flux of particles toward the region where $\delta\theta$ has increased (along the gradient of $\delta\theta$). In other words, a process of negative diffusion should occur here. Any initial large-scale inhomogeneity of $\delta\theta$ increases with time. This is in contrast to the normal diffusion process which results in the formation of homogeneous structures.

II. DIFFUSION COEFFICIENT OF TWO-PHASE MIXTURE

To obtain an explicit term for the negative diffusion coefficient, we consider the simplest lattice system, i.e., the lattice with square symmetry. The values of α and n_∞ can be taken from Refs. 3 and 4, respectively. These are given by

$$\alpha = -a \ln\left(\sinh^{-2}\frac{\varphi}{2}\right) \tag{2}$$

and

$$n_\infty \approx e^{-2|\varphi|}, \tag{3}$$

where a is the lattice constant and φ is the energy of particle-particle interaction measured in units of kT. The approximation shown by $(\approx)$ is valid when $e^{-|\varphi|} \ll 1$. If we deal with the two-phase mixture, the above criterion for φ is fulfilled with sufficient accuracy even for the critical value of the interaction parameter, φ_c. In this case the exponent is given by

$$e^{-|\varphi_c|} \approx e^{-1.76} \approx 0.17.$$

The evolution of particle density in the dilute phase is governed by the continuous equation

$$\partial_t n^{di}(\mathbf{r},t) = -\partial_{\mathbf{r}}\mathbf{j}(\mathbf{r},\mathbf{t}), \tag{4}$$

where $\mathbf{j}(\mathbf{r},\mathbf{t})$ is the density of particle flux in the dilute phase.

Let us multiply both parts of Eq. (4) by $e^{i\mathbf{kr}}$ and integrate over the volume of the dilute phase. Then the left part reduces to

$$\partial_t \int_{di(t)} e^{i\mathbf{kr}} n^{di}(\mathbf{r},t)d\mathbf{r} - \frac{1}{\Delta t}\left(\int_{di(t+\Delta t)} - \int_{di(t)}\right) e^{i\mathbf{kr}} n^{di}(\mathbf{r},t)d\mathbf{r}, \tag{5}$$

where $di(t)$ and $di(t+\Delta t)$ indicate the volumes occupied by the dilute phase at the times t and $t+\Delta t$, respectively, as $\Delta t \to 0$. The first term in Eq. (5) is the time derivative of the Fourier component of the dilute phase density $\partial_t n_{\mathbf{k}}^{di}$ defined by

$$n_{\mathbf{k}}^{di}(t) = \int_{di(t)} e^{i\mathbf{kr}} n^{di}(\mathbf{r},t)d\mathbf{r}. \tag{6}$$

The second term in Eq. (5) describes the effect of the droplet-boundaries displacements during the interval Δt. It can be rewritten in the form

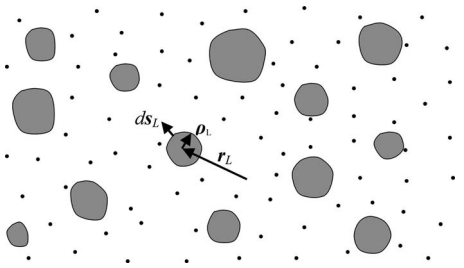

FIG. 1. Schematics of a 2D system undergoing first-order phase transition: droplets of the dense phase (clusters) are shown by gray islands; individual particles are shown by dots.

$$-\sum_L e^{i\mathbf{kr_L}} \int d\mathbf{s_L}\mathbf{j}(\mathbf{r_L}+\rho_\mathbf{L}) n^{di}(\mathbf{r_L}+\rho_\mathbf{L}) e^{i\mathbf{k}\rho_L}, \tag{7}$$

where the integrations are over the surfaces of individual droplets labeled by the index L. The vector $d\mathbf{s}_L$ is oriented outward from the droplet L, as shown in Fig. 1, and $|d\mathbf{s}_L|$ is the element of the Lth surface. The sum runs over all droplets.

After Fourier transforming, the right-hand side of Eq. (4) can be written as

$$\sum_L e^{i\mathbf{kr_L}} \int d\mathbf{s_L}\mathbf{j}(\mathbf{r_L}+\rho_\mathbf{L}) e^{i\mathbf{k}\rho_L} + i\mathbf{k}\int_{di} d\mathbf{r} e^{i\mathbf{kr}}\mathbf{j}(\mathbf{r},t). \tag{8}$$

Similar relationships can be derived for the evolution of the dense phase. Usually, the diffusion of particles within the dense phase can be neglected. Mathematically, this is expressed as

$$\partial_t n^{de}(\mathbf{r},t) = 0, \tag{9}$$

where $n^{de}(\mathbf{r},t)$ is the particle density within the dense phase. Accounting for the evolution of the droplet boundaries, Eq. (9) can be rewritten in the Fourier domain as

$$\partial_t n_{\mathbf{k}}^{de} + \sum_L e^{i\mathbf{kr_L}} \int d\mathbf{s_L} \frac{\mathbf{j}(\mathbf{r_L}+\rho_\mathbf{L})}{1-n_\infty^{di}} e^{i\mathbf{k}\rho_L} = 0, \tag{10}$$

where the definition of $n_{\mathbf{k}}^{de}$ is similar to that given by Eq. (6) but with the integration over the dense phase. The denominator in the integrand of Eq. (10) takes into account the circumstance that not each lattice site is occupied in the dense phase. The condition

$$n^{de} = 1 - n^{di} \approx 1 - n_\infty, \tag{11}$$

which neglects a small capillary effect, is used here (see Ref. 4).

Using Eqs. (5)–(11) and the condition $n_\infty \ll 1$ we arrive at

$$\partial_t n_{\mathbf{k}}^{de} + \partial_t n_{\mathbf{k}}^{di} = -i\mathbf{k}\int_{di} d\mathbf{r} e^{i\mathbf{kr}} D^{di} \partial_{\mathbf{r}} n^{di}(\mathbf{r},t). \tag{12}$$

We have used here the explicit term for the particle flux in the dilute phase given by

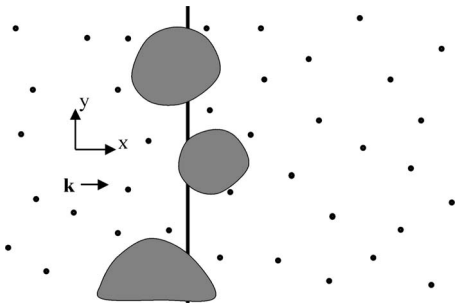

FIG. 2. The integration path along the y axis is shown by the solid line.

$$\mathbf{j} = -D^{di}\partial_{\mathbf{r}} n^{di}(\mathbf{r},t). \tag{13}$$

This means that in the absence of external forces the flux is only due to diffusion in the dilute phase. D^{di} is the diffusion coefficient of the dilute phase, which is considered to be known. In the limiting case, when only the dilute phase is present, the term on the right side of Eq. (12) reduces to $-D^{di}k^2 n_{\mathbf{k}}^{di}$, as in the case of the usual diffusion equation governing the density evolution.

Our purpose is to derive the evolution equation for small inhomogeneous coverage added to the statistically homogeneous system. It should be emphasized that the inhomogeneity scale is chosen to be much greater than the interdroplet distance, i.e., $kl \ll 1$. In this case, the short-range variations of $n^{di}(\mathbf{r},t)$ in Eq. (12) can be neglected, thus simplifying the problem. It looks quite reasonable to assume n^{di} to be dependent on $\mathbf{r}$ through $R^*(\mathbf{r})$: $n^{di}(\mathbf{r}) = n^{di}(R^*(\mathbf{r}))$. Hence,

$$\partial_{\mathbf{r}} n^{di}(\mathbf{r}) \approx \frac{\partial n^{di}(R^*)}{\partial R^*}\frac{\partial R^*}{\partial \theta}\frac{\partial \delta\theta}{\partial \mathbf{r}}. \tag{14}$$

Let us assume that $\delta\theta$ depends on x-coordinate only. Then, considering $\delta\theta$ to be small, we obtain from Eqs. (12) and (14)

$$\partial_t \delta\theta_{\mathbf{k}} \approx -ikD^{di}\frac{\partial n^{di}}{\partial R^*}\frac{\partial R^*}{\partial \theta}\int d\mathbf{r} e^{ikx}\frac{\partial \delta\theta}{\partial x}, \tag{15}$$

where $\delta\theta_{\mathbf{k}} = n_{\mathbf{k}}^{di} + n_{\mathbf{k}}^{de}$. A straightforward integration in Eq. (15) is possible. It is convenient to integrate first over the y-variable as shown in Fig. 2. Thus we have

$$\int d\mathbf{r} e^{ikx}\frac{\partial \delta\theta}{\partial x} = L_y(1-\theta)\int dx e^{ikx}\frac{\partial \delta\theta}{\partial x} = -ik(1-\theta)\delta\theta_{\mathbf{k}}, \tag{16}$$

where L_y is the system size in the y direction.

Using Eqs. (15) and (16) we obtain the final equation for the evolution of the excessive coverage $\delta\theta$ in the form

$$\partial_t \delta\theta_{\mathbf{k}} = -D_{coll}k^2\delta\theta_{\mathbf{k}}, \tag{17}$$

where D_{coll} can be interpreted as the collective diffusion coefficient. It is given by

$$D_{coll} = -D^{di}(1-\theta)\frac{n_\infty \alpha}{R^{*2}}\frac{\partial R^*}{\partial \theta}, \tag{18}$$

where Eq. (1) was used.

Theoretical studies of coarsening kinetics (see, for example, Refs. 5–9) show that the derivative $\frac{\partial R^*}{\partial \theta}$ is positive. The following comments can help to elucidate this point. Let us consider two systems where at some time, t, the radii R^* are equal but the values of θ are different. On average, the distance between droplets in the system with greater θ are smaller than in the other one. Therefore, the redistribution of particles between droplets (as well as cluster growth) is faster in the first case. This shows that $\frac{\partial R^*}{\partial \theta}$ is positive. Hence, the collective diffusion coefficient, D_{coll}, given by Eq. (18), is negative.

A similar expression for D_{coll} can be derived from a rather formal analysis based on the representation of the collective diffusion coefficient in the form

$$D_{coll} = D_J\frac{\partial \mu}{\partial \ln \theta}, \tag{19}$$

where D_{jump} is the jump diffusion coefficient, which describes the particle mobility; μ is the chemical potential of the system. For the model of a 2D lattice gas with NN attraction, considered here, D_{jump} was obtained in Ref. 4. It is given by

$$D_{jump} = D_0\frac{1-\theta}{\theta}n^{di}, \tag{20}$$

where $D_0 \equiv \nu_0 a^2$ and ν_0 are the diffusion coefficient and jump frequency of noninteracting particles, respectively for the Langmuir gas model. [See Eq. (9) in Ref. 4. In real systems, the value of ν_0, being dependent on the temperature, may vary in wide ranges.] In Eq. (20), as previously, we consider $n^{di} \ll 1$ and $n^{di} \approx e^{-2|\varphi|}$.

The derivative $\frac{\partial \mu}{\partial \ln \theta}$, known in the literature as the thermodynamic factor, can be easily obtained from the following analysis. The chemical potential and the density of the dilute phase are related through the condition [see Eq. (3) in Ref. 4]

$$n^{di} = e^{\mu}, \tag{21}$$

which is valid for any rarified gas when the particle-particle interactions are negligible. Using Eqs. (1) and (21) and setting $R = R^*$ in Eq. (1), we can easily obtain

$$\frac{\partial \mu}{\partial \ln \theta} = -\frac{\alpha}{R^{*2}}\theta\frac{\partial R^*}{\partial \theta}. \tag{22}$$

Substituting Eq. (22) into Eq. (19) we obtain

$$D_{coll} = -D_0(1-\theta)\frac{n_\infty \alpha}{R^{*2}}\frac{\partial R^*}{\partial \theta}, \tag{23}$$

that, with regard for $D_0 = D^{di}$, coincides with Eq. (18). One point which should be discussed in more detail is that there is no *a priory* evidence of the applicability of Eq. (19) for the system undergoing phase transition. Strictly speaking, Eq. (19) is valid for equilibrium systems where the relaxation processes have finished. The coincidence of Eqs. (18) and (23) becomes clear if one takes into account that the ripening is a very slow process which occurs under the condition of local equilibrium between different phases. This condition is satisfied during the late stages of ripening.

D_{coll} depends on time through $R^*(t)$. When $R^* \sim t^{1/3}$, the diffusion coefficient behaves as $t^{-1/3}$. Therefore, the effect of negative diffusion is more pronounced when the droplet radii are small.

To obtain an explicit term for D_{coll}, one should specify the dependence $R^*(\theta)$. Its approximate value can be derived for some specific cases. The simplest situation is when some extra material is redistributed among different droplets, assuming that the number of droplets remains constant (the formation of the scaling regime requires much longer time than the diffusion time $D_0 l^{-2}$). For a fixed total number of the droplets, we have $R^* \sim \theta^{1/2}$ and $\frac{\partial R^*}{\partial \theta} = \frac{R^*}{2\theta}$. In this case we have

$$D_{coll} = -\frac{1}{2} D_0 \frac{(1-\theta)}{\theta} \frac{n_\infty \alpha}{R^*}. \tag{24}$$

This formula corresponds to the nonequilibrium droplet-distribution function. After establishing the scaling regime of the droplet evolution, the dependence of R^* on θ becomes more complicated. There were many theoretical attempts to obtain it for small, but still finite, values of θ. The simplest approximation, which can be justified when $\theta \ll 1$, is given by (see the Appendix)

$$R^*(\theta) = \left(\frac{8}{9} \frac{D^{di} n_\infty \alpha}{|\ln \theta|} t \right)^{1/3}. \tag{25}$$

Substituting Eq. (25) into Eq. (23), we obtain

$$D_{coll} = -\frac{1}{3} D_0 \frac{(1-\theta)}{\theta} \frac{n_\infty \alpha}{R^* |\ln \theta|}. \tag{26}$$

This value of D_{coll} is smaller by the coefficient $\frac{3}{2}|\ln \theta|$ than that given by Eq. (24). In the next section, we will use Eqs. (24) and (26) in order to compare them with the results of computer simulations.

III. COMPUTER SIMULATIONS

The purpose of computer simulations is to show the presence of negative diffusion in a macroscopically inhomogeneous lattice-gas system undergoing first-order phase transition. Also, it seems useful to compare the quantitative results of the analytical consideration with the data of Monte Carlo simulations. The comparison can show whether our approach is applicable for studying similar systems with negative diffusion. The consideration of the simplest lattice-gas model with square symmetry and NN interactions makes it possible to compare directly the theoretical and MC data without using any phenomenological or fitting parameters. The diffusion coefficient is obtained in both cases for the same set of the model parameters, namely, the interaction energy φ, coverage θ, and jump frequency ν_0.

Simulations of the particle migration were executed in a system of 130×300 sites. The smaller size is along the x axis. We simulated random jumps of individual particles. The jump probabilities, ν_{ij}, from the occupied ith site to the nearest-neighbor free site j were taken in the form

$$\nu_{ij} = \nu_0 e^{-|\varphi| m_j}, \tag{27}$$

where m_j is the number of NN occupied sites. Jump probability (27) ensures the detailed balance conditions. Also it is consistent with our assumptions that within the dense phase the mass transport can be neglected. It follows from Eq. (27) that the jump probabilities inside dense droplets are proportional to $e^{-3|\varphi|} \to 0$. Other possible models of jump probabilities are discussed in Ref. 10.

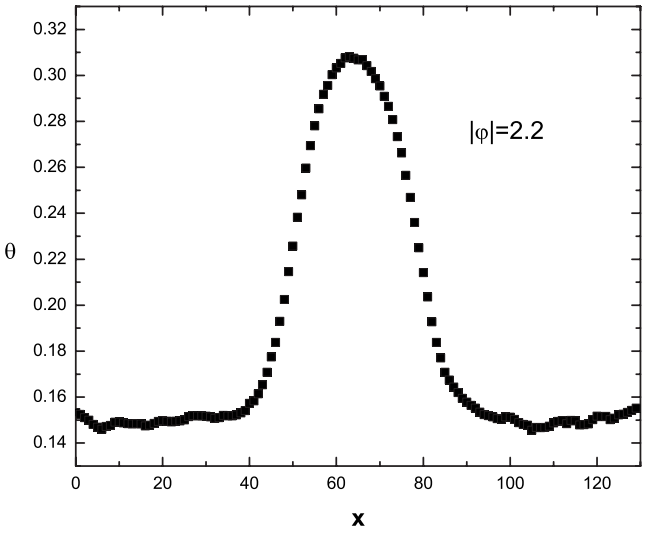

FIG. 3. The coverage profile in the x direction after 38 500 Monte Carlo steps. The data are averaged over 1000 individual runs.

The computer time was monitored in units of Monte Carlo steps (MCS). Each MC step corresponds to $(4\nu_0)^{-1}$ of real time, t, i.e., the time used in the theoretical part. In the course of one MCS, each lattice site is interrogated once on average for the probability of a particle to jump out of it. More details are given in Refs. 11–14.

To show that at undercritical temperatures the particle flux is along the gradient of θ (the uphill flux) we have used the following scheme for the computer simulations. Initially, particles were randomly arranged on the lattice with average coverage $\theta = 0.15$. Then they were allowed to jump with probabilities given by Eq. (27). The total number of particles is constant during 20 000 MCS. After that, the extra material $\delta\theta = 0.15$ was added gradually (one particle per 10 MCS) to the central strip of size 30×300, thus providing the macroscopically inhomogeneous coverage distribution: $\theta = \theta(x)$. This process lasted for an additional 13 500 MCS. The regime of low deposition rate prevents the formation of new clusters. After that, the inhomogeneous system evolved for an extra 10 000 MCS. Hence, the overall simulation time for an individual run was equal to 43 500 MCS.

Figure 3 illustrates a typical coverage distribution after 38 500 MCS. The x coordinate is given in units of the lattice constant a. In the central area close to $x = 65$ the total number of particles were increasing when $|\varphi| > \varphi_c$. We calculated the increase of the particle numbers, ΔN, inside the region $53 \leq x \leq 77$ for the last 5000 MCS. The coverage distribution after 43 500 MCS is very similar to that shown in Fig. 3 (the two are almost indistinguishable by eye due to the small time interval between them).

Considering the fluxes at the boundaries of the selected region to be governed by the diffusion mechanism, we can express ΔN as

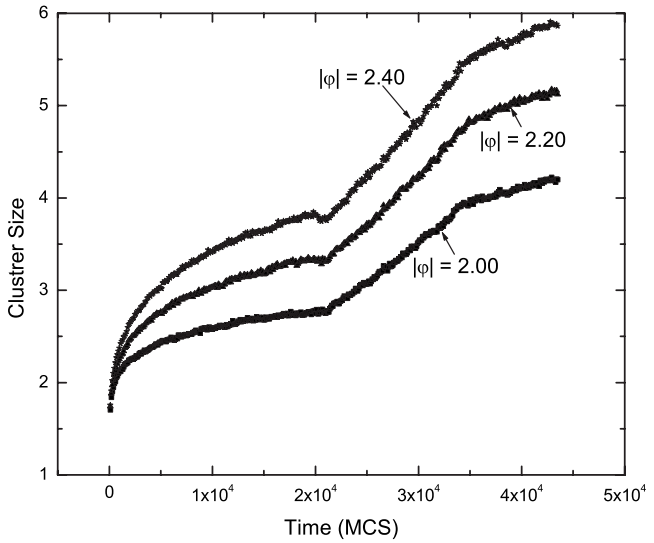

FIG. 4. The dependence of the average cluster size on time for three different values of interaction parameter φ; $x=53$. The linear dependence in the range of 20 000–33 500 MCS is due to the constant flux of extra particles which dominates the quasiequilibrium ripening mechanism resulting in $t^{1/3}$ growth law.

$$\Delta N = -\left\{\left(D_{coll}\frac{\partial\theta}{\partial x}\right)\Big|_{x=53} - \left(D_{coll}\frac{\partial\theta}{\partial x}\right)\Big|_{x=77}\right\} * 300 * 5000/(4\nu_0), \quad (28)$$

where the factors 300 and $5000/(4\nu_0)$ signify the length of the stripe and the measurement time, respectively. Equation (28) is applicable for obtaining the diffusion coefficients if only insignificant variations of the coverages and their gradients in the region $53 \le x \le 77$ occur during the time interval of 5000 MCS. This condition is satisfied for all calculations presented below.

Taking into account that the values of D_{coll} and $|\frac{\partial\theta}{\partial x}|$ at symmetric points $x=53$ and $x=77$ should be equal to each other, it is possible to use Eq. (28) for obtaining the diffusion coefficient [it can be easily seen from Eq. (28) that $D_{coll} < 0$ if $\Delta N > 0$].

To compare analytical expressions (24) and (26) with the diffusion coefficients, obtained from MC simulations of the material transfer [i.e., obtained using Eq. (28)], the information about R^* is required. Approximately, R^* can be considered to be equal to the average value of the cluster radius, $\bar{R}$. The values of $\bar{R}$ and the average cluster size, L_{cl}, shown in Fig. 4, are related through the equation $\bar{R}=\frac{2}{\pi}\times L_{cl}$. The quantity L_{cl} was defined as the ratio of the number of occupied lattice sites along the thick line, shown in Fig. 2, to the total number of clusters crossed by it.

L_{cl} was calculated by averaging over 1000 individual runs for the strips $x=53$ and $x=77$. We can see an essentially different behavior of $L_{cl}(t)$ inside three specific time intervals where (i) the initial clusters grow, (ii) the new particles are deposited, and (iii) the evolution of inhomogeneous coverage occurs.

Figure 5 shows the diffusion coefficients obtained from

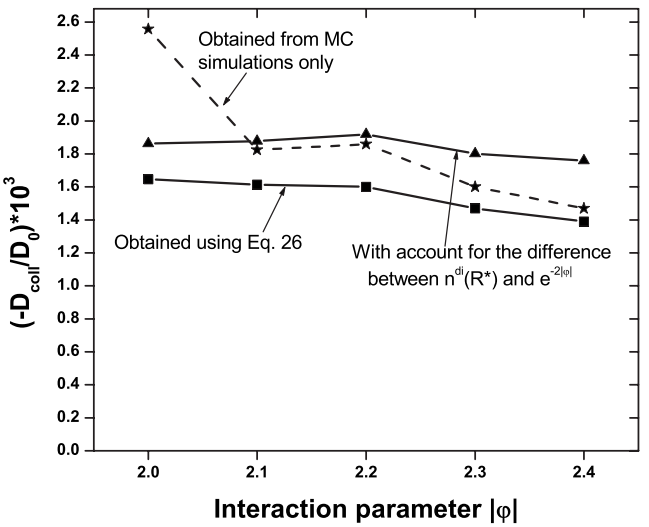

FIG. 5. The diffusion coefficients obtained for five different values of the interaction parameter φ; $x=53;77$. The lines serve for visual convenience only.

both the MC simulations (stars) and the ones calculated using Eq. (26) (squares). We studied the mass transfer through the boundaries $x=53$ and $x=77$ into the central region during the time interval 43500–38500=5000 (MCS). The values of R^* were obtained in the central point of this interval. We see quite good agreement of the data with the exception of the values for $|\varphi|=2.0$. The disagreement in this point (about 36%) may be attributed to the close vicinity of the interaction parameter to the critical value. The accuracy of the value n_∞ ($n_\infty \approx e^{-2|\varphi|}$) in this case is not too good. A better agreement can be achieved if we change n_∞ by the value $e^{-2|\varphi|}e^{\alpha/R^*}$. The last factor takes into account the increase of the dilute phase concentration due to the finite radii of the droplets. The triangles show the modified diffusion coefficients with account for this correction. In this case, the disagreement at $|\varphi|=2$ is less (about 27%). Maybe, the agreement of theoretical and MC data could be better if the variation of the coverage with the distance will be smoother to guarantee the linear response regime of the evolution (see, for example, simulations in Ref. 15). In this case the simulation procedure will require larger lattice-gas system and much more simulation time.

The theoretical diffusion coefficients obtained from Eq. (24) are approximately two times greater than those in Fig. 5. This shows that in the time interval [38500,43500] the diffusion proceeds under conditions of quasiequilibrium rather than in the nonequilibrium regime which was assumed in course of the derivation of Eq. (24).

IV. CONCLUSION

The phenomenon of negative diffusion (see, for example, Refs. 16–18) is known in the literature for a long time. The mechanism, described here, is caused by the natural tendency to minimize the free energy in course of the first-order phase transition that is the continuation of the spinodal decomposition at late stages of the two-phase separation (Ref.

19), and evolves without the interference of any external force. Our theory can be improved further in the part that concerns the choice of a more realistic physical model for obtaining the dependence $R^*(t,\theta)$. The scheme of the computer simulations, outlined above, is not common for the lattice-gas systems. In contrast to papers (Refs. 4, 11, and 12) where the center-of-mass particle displacements were studied, the present MC procedure deals with the particle flux caused by the gradient of coverage. We start from mimicking the microscopic random displacements of individual particles resulting in the formation of macroscopic fluxes described by the diffusion coefficients. This approach which gives the possibility of direct numeric calculations of the collective diffusion coefficients contradicts the computer simulations in Refs. 4, 11, and 12. In these studies the particle mobilities (jump diffusion coefficients) were obtained from microscopic dynamics unlike the collective diffusion coefficients.

It was not within our purpose to develop a complete or universal theory of diffusion in systems with ripening. Nevertheless, in three dimensions and in systems with greater radii of particle-particle interactions, the qualitative physical picture and theoretical analysis may be very similar to ours.

The phenomenon of negative diffusion can be responsible for the evolution of nanostructures. In this context, it can be used to reduce the manufacturing cost of nanostructures with complex geometries.

ACKNOWLEDGMENT

This work was partially supported by Ukrainian project VTS (Project No. VTS/138) (Nanophysics).

APPENDIX

To derive Eq. (25), we will follow the general scheme of the Lifshitz-Slyozov theory modified for two-dimensional system. The steady-state limit for the concentration $n^{di}(\mathbf{r})$ is given by

$$\frac{\partial^2 n^{di}}{\partial \mathbf{r}^2} = 0, \tag{A1}$$

which follows from the continuity equation where the term $\partial n^{di}/\partial t$ is neglected. Using Eq. (1), the boundary conditions can be written as

$$n^{di}(\mathbf{r_L} + \rho_\mathbf{L}) = n_\infty(1 + \alpha/R_L), \tag{A2}$$

where R_L is the radius of the Lth cluster. If only single droplet is available, the solution of Eq. (A1) is given by

$$n^{di}(r) = c_0 + c_1 \ln r. \tag{A3}$$

Taking into account the boundary condition (A2) at $r=R$ and at arbitrary distance $r=r_b$, given by $n^{di}(r_b)=n^*$, it is possible to obtain the two constants c_0 and c_1. The changes of the droplet radius, R, are given by the balance equation

$$\frac{\partial R}{\partial t} = D^{di}\frac{\partial n^{di}(r)}{\partial r}\bigg|_{r=R}. \tag{A4}$$

The radius R increases or decreases with time whether or not the concentration $n^{di}(r_b)$ is greater or smaller than $n^{di}(R)$.

If we deal with an ensemble of droplets, the situation is more complicated. But again, in close vicinity to a given droplet the value n^{di} is determined by Eq. (A2) that does not depend on the surroundings. Far from it, $n^{di}(\mathbf{r})$ depends rather on the positions of the other droplets than that of a given one and it is reasonable to consider n^{di} to be independent of $\mathbf{r}$, i.e., $n^{di}(|\mathbf{r}=r_b|)=n(r_b)=n(R^*)$, where $r_b=R^*/\sqrt{\theta}$. For this choice of r_b, the droplets with $R=R^*$ are neither growing, nor shrinking as it was assumed in the Introduction.

Using Eqs. (A2)–(A4), we obtain

$$\frac{\partial R}{\partial t} = \frac{p}{1 + \dfrac{\ln(R/R^*)}{\ln\sqrt{\theta}}}\left(\frac{1}{R^*} - \frac{1}{R}\right)\frac{1}{R}, \tag{A5}$$

where $p=D^{di}n_\infty\alpha/|\ln\sqrt{\theta}|$. It is convenient to introduce new variables

$$t' = pt, \quad \tau = 3\ln R^*(t), \quad u = R/R^*.$$

Then the rate Eq. (A5) can be rewritten in terms of the new variables as

$$\frac{\partial u^3}{\partial \tau} = \frac{u-1}{R^{*2}\dfrac{dR^*}{dt'}(1 + \ln u/\ln\sqrt{\theta})} - u^3. \tag{A6}$$

For small values of θ, Eq. (A6) can be simplified by neglecting the second term in the brackets of the denominator. In this case the problem reduces to the Lifshitz-Slyozov theory. The difference is only in the definition of the constant p, which in our case has the extra factor $|\ln\sqrt{\theta}|^{-1}$. Repeating the arguments of Lifshitz and Slyozov (Refs. 1 and 2) we can easily obtain the dependence $R^*(\theta,t)$. It is given by

$$R^* = \left(\frac{4}{9}pt\right)^{1/3} = \left(\frac{8}{9}\frac{D^{di}n_\infty\alpha}{|\ln\theta|}t\right)^{1/3}. \tag{A7}$$

It follows from (A7) that in contrast to the three-dimensional case, the dependence of R^* on θ in the range of small θ cannot be neglected. At the same time, in the course of derivation of Eq. (A7) we have assumed tacitly that $\theta > n_\infty$. This imposes the restriction on the validity of Eq. (A7) also from the side of very small θ, which are not considered in the present work.

[1] I. M. Lifshitz and V. V. Slyozov, J. Phys. Chem. Solids **19**, 35 (1961).
[2] E. M. Lifshitz and L. P. Pitaevskii, *Physical Kinetics* (Pergamon, London, 1981).
[3] R. J. Baxter, *Exactly Solved Models in Statistical Mechanics* (Academic Press, London, New York, 1982).
[4] A. A. Chumak and C. Uebing, Surf. Sci. **476**, 129 (2001).
[5] A. J. Ardell, Metall. Trans. **3**, 1395 (1972); Acta Mater. **20**, 61 (1972).
[6] J. A. Marqusee and J. Ross, J. Chem. Phys. **80**, 536 (1984).
[7] J. A. Marqusee, J. Chem. Phys. **81**, 976 (1984).
[8] M. Tokuyama and Y. Enomoto, Phys. Rev. E **47**, 1156 (1993).
[9] J. H. Yao, K. R. Elder, H. Guo, and M. Grant, Phys. Rev. B **47**, 14110 (1993).
[10] A. Sadiq and K. Binder, Surf. Sci. **128**, 350 (1983).
[11] A. A. Chumak and C. Uebing, Eur. Phys. J. B **9**, 323 (1999).
[12] P. Argyrakis and A. A. Chumak, Phys. Rev. B **66**, 054303 (2002).
[13] P. Argyrakis, A. A. Chumak, and M. Maragakis, Phys. Rev. B **71**, 224304 (2005).
[14] P. Argyrakis, A. A. Chumak, and M. Maragakis, Phys. Rev. B **76**, 054209 (2007).
[15] K. W. Kehr, K. Binder, and S. M. Reulein, Phys. Rev. B **39**, 4891 (1989).
[16] W. S. Gorsky, Phys. Z. Sowjetunion **8**, 457 (1935).
[17] V. G. Karpov, Phys. Rev. Lett. **75**, 2702 (1995).
[18] N. N. Christov, Europhys. Lett. **36**, 687 (1996).
[19] K. Binder and P. Fratzl, in *Phase Transformations in Materials*, edited by G. Kostorz (Wiley-VCH, Weinheim, 2001), p. 409.